

Manufacturing Letters

MANUFACTIONS

Manufacturing Letters 00 (2022) 000-000

50th SME North American Manufacturing Research Conference (NAMRC 50, 2022)

Experimental and simulative analysis of an adapted methodology for decoupling tool wear in end milling

Nils Potthoff^{a,*}, Ankit Agarwal^b, Florian Wöste^a, Jan Liß^a, Laine Mears^b, Petra Wiederkehr^a

^aVirtual Machining, TU Dortmund University, Otto-Hahn-Straße 12, 44227 Dortmund, Germany ^bInternational Center for Automotive Research, Clemson University, Greenville, SC 29607

* Corresponding author. Tel.: +49-231-755-5819; fax: +49-231-755-7936. E-mail address: nils.potthoff@tu-dortmund.de

Abstract

The machining of nickel-based superalloys such as Inconel 718 still poses a great challenge. The high strength and temperature resistance of these materials lead to poor machinability, resulting in high process forces and extensive tool wear. However, this wear is stochastic when reaching a certain point and is difficult to predict. To generate consistent wear conditions, the tool wear can be decoupled from the milling process by creating artificial wear using grinding. In this paper, a multi-axis approach for decoupling tool wear is presented and analyzed. Therefore, scanning electron microscope images of different wear states – worn and artificially worn – are analyzed. In addition, the occurring process forces of naturally and contrived worn inserts are compared in orthogonal cutting experiments as an analogy setup. Finally, a finite element analysis using a novel methodology for segmenting relevant cutting edge sections using digital microscope images provides qualitative insights on the influence of different wear conditions.

© 2022 Society of Manufacturing Engineers (SME). Published by Elsevier Ltd. All rights reserved. This is an open access article under the CC BY-NC-ND license (http://creativecommons.org/licenses/by-nc-nd/4.0/) Peer-review under responsibility of the Scientific Committee of NAMRI/SME.

Keywords: End Milling; Tool Wear; Decoupling Wear; Inconel 718

1. Introduction

Nickel-based superalloys have high strength, corrosion and temperature resistance. These properties make them particularly attractive for the energy sector and for the aerospace industry [1, 2]. However, the advantages of these properties make the materials difficult to machine. The resulting high process forces lead to rapid tool wear [3–5]. In this regard, short tool life was identified, especially when machining Inconel 718 (IN718) [6]. Therefore, many studies analyzed the tool wear behavior for different processes, e.g. turning [7], end milling [8, 9], or micro-milling [10]. Alternative path strategies such as trochoidal milling [11] and different cutting speeds [12] have been investigated to improve productivity. The influence of varying cutting conditions was analyzed taking the occurring tool wear into account [11]. In this context, studies were conducted to address the stochastic nature of the wear progression [13]. In order to optimize the machining processes, simulation-based analyses can be used. In literature, different approaches for taking tool wear into account using finite element simulations are presented [14, 15]. Bergmann et al. [16] introduced a model for wear-dependent prediction of process forces used in a physically-based simulation system. For increasing the precision of these models, accurately configurable testing conditions are necessary. In order to avoid time-consuming and cost-intensive test, [17, 18] presented an approach to artificially generate tool wear and, thus, decouple it from the machining process. However, the method of generating artificial wear by grinding needs further improvement to increase accuracy and reproducibility, especially regarding the wear shape and the resulting process forces.

Based on the work presented in [17], an adapted methodology for decoupling tool wear will be discussed in the following. First, a multi-axis approach for grinding inserts was used for precise positioning using multiple sensors, followed by the evaluation of the reproducibility based on the flank wear width of the cutting edge. Subsequently, a visual analysis was carried out using scanning electron microscope (SEM) images to in-

vestigate the deviation between naturally worn and artificially worn inserts in different wear states. The method of creating contrived inserts was validated utilizing an analogy experiment in which the occurring process forces were measured and compared to those of the naturally worn inserts. By means of digitized cutting inserts, a new method for the extraction of profiles is presented taking tool wear into account, which was used for a subsequent FEA. Finally, a qualitative analysis of profiles of a new, naturally worn, and artificially worn insert on the resulting chip formation as well as the cutting and normal forces is conducted.

2. Methodology for decoupling tool wear

The high tool wear involved in the machining of Inconel 718 is stochastically influenced. In order to examine the tool wear in detail, inserts have been artificially worn by grinding. Due to this, reproducible wear states could be generated. However, previous investigations [17] have shown that the approach used is only suitable to a limited extent for the generation of artificial wear, especially regarding the reproducability. Therefore, a new methodology is presented that extends the previous approach by using mutli-axes grinding. Furthermore, the material and machines used are specified and the results are analyzed.

2.1. Analysis of the cutting edge displacement

When milling Inconel 718, a superposition of abrasive and adhesive wear occurs (initial stage and steady-state stage) up to tool failure (collapse stage) [19]. This wear results in a shape deviation of the initial cutting edge. To determine this displacement, the tool wear of nine inserts with flank wear widths of VB = 150 μ m, VB = 300 μ m, and VB = 450 μ m was each analyzed using a digital microscope (Keyence VHX-950F). In order to induce tool wear, a cutting velocity of $v_c = 40 \, \text{m min}^{-1}$, a feed per tooth of $f_z = 0.09 \, \text{mm}$, a depth of cut and width of cut of $a_p = a_e = 1 \, \text{mm}$ was chosen for all experiments. The microscope images were taken in the tool reference plane and the angle between the major cutting edge and the displaced tool corner was measured. Fig. 1 shows an example of the measurement of the wear dependent angle. As result an angle of approx. $13.73^{\circ}\pm0.51$ was determined for all inserts.

2.2. Creating artificial wear using multi-axis grinding

In order to generate artificial tool wear, inserts were prepared on a 5-axis dressing machine of the type Geiger AP-800 Fusion.

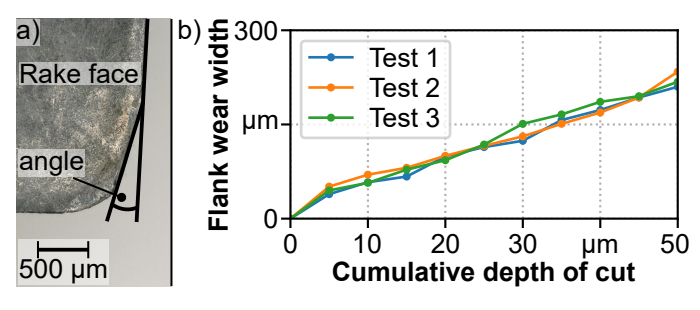


Fig. 1. a) Measurement of the angle between the major cutting edge and the displaced tool corner in the tool reference plan. b) Comparison of the repeatability of the artificially generated flank wear width

The tool used was a square shoulder milling cutter with carbide inserts (Sandvik Coromant R390-11 T3 08M-PM 1130) with multilayer AlTiCrN coating. The experimental setup is shown in Fig. 2. The silicon carbide (SiC) grinding wheel with resinoid bonding and the tool were aligned using a camera system and an acoustic emission sensor for contact detection to ensure precise positioning.

In order to investigate the reproducibility, three experiments were conducted under the same conditions. For reaching different wear states, a width of cut of $a_{\rm e}=1$ mm and a depth of cut of $a_{\rm p}=5\,\mu{\rm m}$ per infeed was used. The spindle speed of the grinding wheel was set to $n_{\rm g}=1000\,{\rm RPM}$ and the opposed rotating tool speed was set to $n_{\rm t}=600\,{\rm RPM}$. For each test, a new insert was applied. Fig. 1b shows the generated flank wear width over the cumulative depth of cut. The results show that the multi-axis approach could produce consistent flank wear widths. Since the determination of the flank wear width is partly based on experience, a more detailed analysis of the surface topography is necessary.

2.3. Analysis of the cutting edge topography

In order to evaluate the generated inserts, the relevant areas were analyzed using scanning electron micrographs (Tescan, Mira III XMU). SEM images of the naturally worn inserts were compared to the respective artificially generated states in Fig. 3. It can be seen that the shape of the flank wear could be adequately reproduced. Nevertheless, the measurements show that the naturally worn inserts had slightly abrasive wear along the entire engagement width, which occurred after the initial wear of the tool. The surface topographies of the naturally worn inserts showed a preferred direction, which is represented by scratches/grooves parallel to the cutting direction. These could be generated to a similar extent using the grinding wheel (cf. Fig. 3, VB 150), although material smearing could be detected on the naturally worn inserts of VB 300 and VB 450.

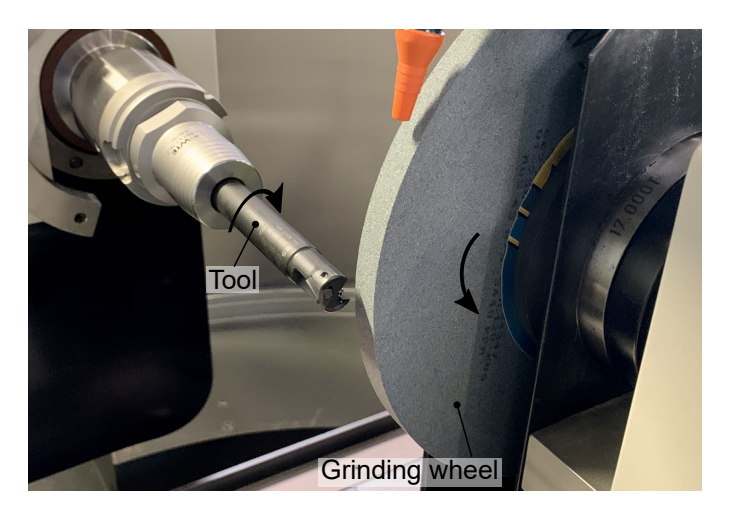


Fig. 2. Experimental setup of multi-axis grinding

Fig. 3. SEM images of different wear states (VB = 150 $\mu m,~VB = 300 \,\mu m,$ VB = $450 \,\mu m)$

3. Experimental setup and analysis

Validation tests were conducted in order to analyze the resulting process forces. In the following, the analogy test setup used is presented and the process forces of the naturally worn and contrived inserts are analyzed.

3.1. Analogy test setup

The influence of the artificially generated inserts on the process forces was analyzed using analogy experiments. For this purpose, the nickel-based superalloy IN718 was machined on a three-axis machine tool specifically built for the conduction of orthogonal cutting experiments. Orthogonal cutting experiments were conducted to fundamentally investigate the machining process. The influence of the artificially generated inserts on the process forces was analyzed. The nickel-based superalloy IN718 was used as the workpiece material. The previously analyzed inserts with different wear conditions were used for the experiments. The process was designed with only the peripheral cutting edge of the tool engaged in order to avoid the influence of the minor cutting edge on the process forces. For this purpose, a depth of cut of $a_p = 1$ mm was used. The resulting forces were measured using a three-component dynamometer (Kistler 9263). A surface speed of the workpiece of $v_c = 40 \,\mathrm{m\,min^{-1}}$ was used to ensure the comparability to milling experiments. The schematic experimental setup is depicted in Fig. 4a. In addition, a detailed view of the experiment (cf. Fig. 4b) as well as the chip formation (Fig. 4c) and the resulting chip (Fig. 4d) are presented. Before each test, a finishing cut was conducted with a new insert to guarantee reproducible engagement situations. After this, the insert was replaced with a prepared - naturally worn or contrived - insert.

3.2. Process force analysis

In order to validate whether multi-axis grinding of inserts is suitable for decoupling tool wear from the machining process, the resulting process forces were investigated. Using the aforementioned dynamometer, the forces were measured in cutting and normal direction with a sampling rate of $f_{\rm meas}=100\,000\,{\rm Hz}$. To ensure the transferability of the results obtained in the analogy setup onto the milling process, the width of cut was adapted according to the feed per tooth of the milling process to $a_{\rm e}=0.09\,{\rm mm}$. Fig. 5 shows the cutting and normal forces for flank wear widths of VB = 150 $\mu{\rm m}$, VB = 300 $\mu{\rm m}$, and VB = 450 $\mu{\rm m}$. Additionally, a distinction between naturally worn and contrived inserts is depicted.

For the wear state of VB = $150\,\mu\text{m}$, the process forces in cutting direction showed a good correspondence and a deviation of $\Delta F_c = 6\,\text{N}$ on average. In contrast, the normal forces had a higher mean difference of $\Delta F_n = 52\,\text{N}$. The deviation in the normal forces can be explained by the initial wear along the cutting edge which is noticeable by the slightly abrasive wear and, therefore, a cutting edge rounding (cf. Fig. 3). This resulted in much more consistent wear of the naturally worn

Fig. 4. a) Schematic experimental setup of the orthogonally cutting test. b) Detailed view of the experimental setup with c) chip formation and d) exemplary resulting chip

insert, whereas the grinding process produced sharp edges between the artificially worn and non-worn areas. Initial wear had a comparatively positive effect on the forces, particularly in normal direction. The comparison with the cutting and normal forces measured using a new insert shows that the wear tended to lead to increased process forces. Fig. 6 illustrates the resulting forces with a new tool and the particular mean values. The mean value of the cutting force was $F_c = 367 \,\mathrm{N}$ and the force in normal direction was $F_n = 231 \,\mathrm{N}$. These process forces are used to classify the occurring forces of the worn inserts. When considering the resulting process forces of the wear condition $VB = 300 \,\mu m$, the mean values of the cutting forces vary only slightly ($\Delta F_c = 25 \text{ N}$), whereas the normal forces differ significantly. For the process with the naturally worn inserts, an average normal force of $F_{n,R} = 281 \text{ N}$ occurred, which was significantly lower than the corresponding cutting force. The process forces of the contrived inserts behaved oppositely. Here, the resulting normal force was on average $F_{n,CA} = 433 \text{ N}$ and, thus, 30 N higher than the cutting force. This suggests that, especially with increasing flank wear widths, the ground area on the flank face becomes too large compared to the natural wear that occurred, resulting in a significantly higher level of the normal force. A comparison with the SEM images of the wear condition VB 300 (cf. Fig. 3) confirms this thesis. The resulting mean value of the normal force of the contrived insert with a flank wear width of 450 µm showed the same behavior with $F_{\rm n} = 772 \,\rm N$ almost twice as high as the forces in normal direction of the naturally worn insert. For the cutting forces, however, a smaller difference (49 N) was found between the naturally worn and contrived inserts. The evaluation of the process forces showed that the multi-axis approach led to a good reproducibility with regard to the cutting forces. In contrast, the normal forces deviated significantly from the corresponding forces of the worn inserts.

4. Simulation of segmented cutting sections

For the detailed analysis, additional FE analyses were conducted. In order to generate the corresponding tool models for the 2D FE analyses, an approach was developed taking the wear-dependent geometry of the inserts into account. In this section, an orthogonally cut will be simulated and the resulting cutting and normal forces will be analyzed.

4.1. Cutting edge segmentation

For segmenting cutting sections, the inserts were initially digitized. Consequently, a confocal microscope (Confovis ToolInspect) was used to measure areas of the naturally worn and artificially worn inserts. In addition to the detection of the worn areas, the measured sections were selected to allow for an alignment by means of the rake face and flank face. Using the software gom inspect, the correct positioning of the measured data of the naturally worn and contrived cutting edge was achieved by an initial alignment, followed by a local best-fit. This ensured the segmentation was carried out at the same position. Fig. 7 shows the aligned cutting inserts of the wear condition VB 150. The digitized naturally worn insert is presented as a gray surface mesh and the contrived insert as a blue point

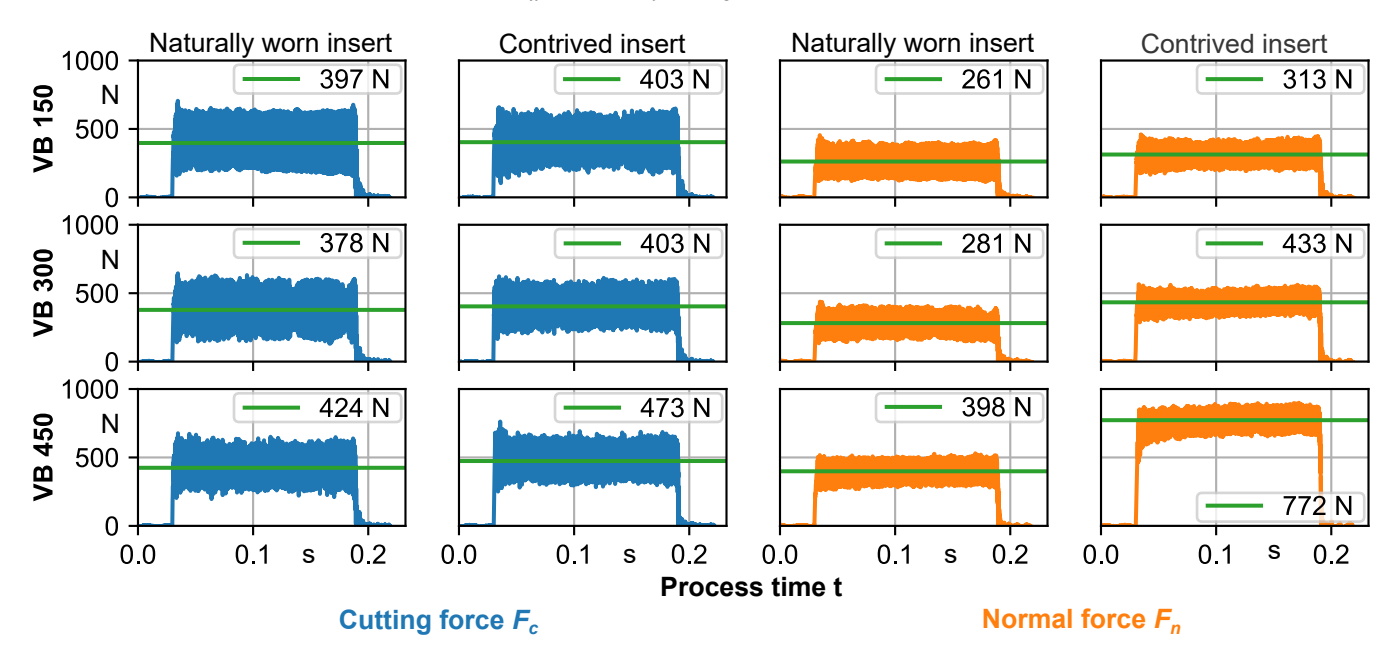


Fig. 5. Normal force (F_n) and cutting force (F_c) of orthogonally cutting experiments of the naturally worn and the contrived inserts with different wear states $(VB = 150 \,\mu\text{m}, VB = 300 \,\mu\text{m}, VB = 450 \,\mu\text{m})$. Additionally, the mean value is displayed in green.

Fig. 6. Process forces in cutting and normal direction with a new insert and its mean value in green

Fig. 8. a) Extraction of a profile of a digitized cutting insert with a flank wear width of VB = $150\,\mu m$ and b) 2D-projection of extracted profiles of new, natural wear, and contrived wear state

cloud. Particularly in the wear area, a clear deviation from each other can be recognized.

For analyzing the influence of different shapes of the cutting edge, a representative section of the worn area was chosen. In the first step, a profile of each wear state (natural and artificial) was extracted. For reference, the profile of a new insert was also segmented. A schematic illustration of the extraction is depicted in Fig. 8a. Further, Fig. 8b shows the overlaid profiles of a new, a naturally worn and an artificially worn insert with a flank wear width of VB = $150 \,\mu\text{m}$. The significant displacement of the cutting edge of the worn inserts compared to a new insert can be seen. In contrast, the geometric deviation between naturally worn and artificially worn insert is rather small and indicates a good accordance. In the next step, the generated profiles were extruded to a width of $w = 40 \,\mu\text{m}$ and utilized for an FEA to qualitatively evaluate the occurring process forces.

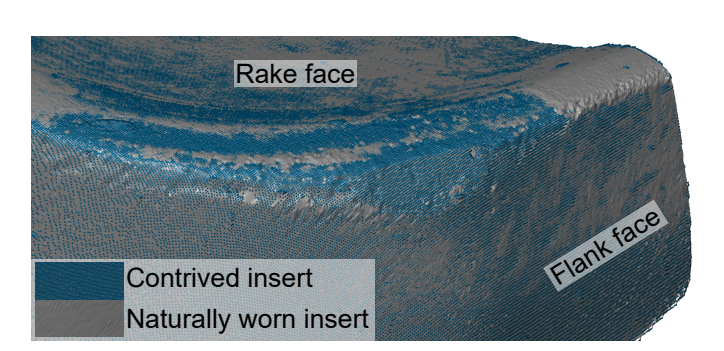


Fig. 7. Alignment of naturally and artificial worn insert with a flank wear width of VB = $150\,\mu m$

4.2. Finite element analysis

For a qualitative analysis of the artificially worn inserts on a local scale, FE simulations were conducted allowing for a comparison between a contrived and a naturally worn insert, each with a flank wear width of $VB = 150 \,\mu m$ (cf. Fig. 9). As a reference, the chip formation process for a new insert was also considered. Within these simulations, an analogy model was implemented, which allows the execution of orthogonal cuts by assuming plane strain cutting conditions. As the modeling approach, the Coupled Eulerian Lagrangian (CEL) [20] method was applied as implemented in the commercial FE software Abaqus/Explicit. In this context, the workpiece was described by an Eulerian and the tool, which was assumed to be rigid, by a Lagrangian formulation. The workpiece model was discretized using coupled temperature-displacement elements of the type EC3D8RT with a minimum length of 5 µm in the area adjacent to the engagement. The applicability of the CEL method to model orthogonal metal cutting has been demonstrated in [21]. To model the material response of the workpiece, the constitutive law by Johnson and Cook was applied to account for the influence of strain hardening, the strain rate and thermal softening [22]. The corresponding parameter



Fig. 9. FE-analysis of a naturally worn and a contrived insert with a flank wear width of VB = $150\,\mu m$ compared to a new insert

values were adopted from [23] for the nickel-based superalloy IN718. The friction between the tool and the workpiece was modeled using Coulomb friction law with a constant coefficient of $\mu=0.36$ [23]. In accordance with the experiments, a cutting velocity of $v_c=40\,\mathrm{m\,min^{-1}}$ and a undeformed chip thickness of $h_{\mathrm{cu}}=90\,\mu\mathrm{m}$ were defined. Due to the flank wear width of VB = 150 $\mu\mathrm{m}$ present at the naturally worn and contrived cutting edge, the chip formation process is significantly influenced compared to the new insert. The separation of material occurred further above, which is indicated by the comparatively smaller thickness of the chip, especially in the case of the naturally worn insert. As a result, strong ploughing effects occurred, as a large part of the workpiece material was pressed under the cutting edge due to the negative rake angles.

The simulated forces of each wear condition are compared in Fig. 10. It can bee seen that the cutting and normal forces strongly increased resulting by the chip formation. The simulation of the new inserts resulted in a lower normal force level compared to the cutting force. In contrast, both worn conditions showed a similar level for both, cutting force and normal force. From these results it can be concluded that the geometry of the cutting edge, especially for a worn state, has a negative effect on the normal forces. Due to the changed geometry, a displacement of the material separation took place, which induced higher normal forces.

A comparison of the experimentally measured and the simulated process forces shows a considerably smaller force level. This is due to the simplified assumptions of the modeling and the different contact situation. While the forces of the entire engagement width were measured in the experiments, only a small representative section was used in the simulation. Nevertheless, a wear-dependent increase of the forces can be observed.

5. Conclusion

In this paper, a multi-axis approach was used to generate artificially worn inserts by grinding. With the presented methodology, reproducible wear conditions could be created. The precision of the positioning was significantly improved by using a camera system and an acoustic emission sensor. A visual comparison of SEM images of naturally worn and artificially worn inserts showed good accordance with the shape of the wear states. However, deviations with an increase of the flank wear width, especially regarding the initial wear along the cutting edge, could be demonstrated. To validate the contrived inserts, experiments were carried out on an analogy test setup. The analysis of the resulting forces showed a similar force level of the cutting forces of various wear conditions of the naturally worn and contrived inserts and, consequently, could be reproduced well. The average of the normal forces differed significantly with increasing wear, which could be explained by the differences of the initial wear along the cutting edge between naturally worn and contrived inserts. A new method for extracting profiles from digitized inserts of different wear conditions served as a basis for an FE simulation. With these profiles, a

Fig. 10. Resulting cutting and normal forces (F'_c, F'_n) of the FEA with a flank wear width of VB = 150 μ m compared to a new insert

qualitative analysis was conducted to investigate the influence of different cutting edge geometries on chip formation and the resulting process forces.

In future investigations, the multi-axis approach will be extended to include initial wear along the cutting edge. Furthermore, the extracted profiles and the FEA will be used to determine specific cutting force coefficients for different wear conditions, which will then be used in a geometric physically-based simulation system to calculate the process forces.

Acknowledgements

The investigations are based on the research project "Stochastic Modeling of the Interaction of Tool Wear and the Machining Affected Zone in Nickel-Based Superalloys and Application in Dynamic Stability", which is kindly funded by the German Research Foundation (DFG – 400845424) and the National Science Foundation under Grant No. 1760809. Any opinions, findings, and conclusions or recommendations expressed in this material are those of the authors and do not necessarily reflect the views of the National Science Foundation.

References

- [1] Wu BH, Zheng CY, Luo M, and He XD. Investigation of trochoidal milling nickel-based superalloy. In *Materials Science Forum*, volume 723, pages 332–336. Trans Tech Publ, 2012.
- [2] Thakur A and Gangopadhyay S. State-of-the-art in surface integrity in machining of nickel-based super alloys. *International Journal of Machine Tools and Manufacture*, 100:25–54, 2016.
- [3] Ulutan D and Ozel T. Machining induced surface integrity in titanium and nickel alloys: A review. *International Journal of Machine Tools and Manufacture*, 51(3):250–280, 2011.
- [4] Ezugwu EO and Pashby IR. High speed milling of nickel-based superalloys. *Journal of materials processing technology*, 33(4):429–437, 1992.
- [5] Ezugwu EO, Wang ZM, and Machado AR. The machinability of nickel-based alloys: a review. *Journal of Materials Processing Technology*, 86(1-3):1–16, 1999.
- [6] Anthony Xavior M, Manohar M, Jeyapandiarajan P, and Madhukar PM. Tool wear assessment during machining of inconel 718. Procedia engineering, 174:1000–1008, 2017.
- [7] Cantero JL, Díaz-Álvarez J, Miguélez MH, and Marín NC. Analysis of tool wear patterns in finishing turning of Inconel 718. Wear, 297(1-2):885–894, 2013.
- [8] Li HZ, Zeng H, and Chen XQ. An experimental study of tool wear and cutting force variation in the end milling of inconel 718 with coated carbide inserts. *Journal of Materials Processing Technology*, 180(1-3):296–304, 2006.
- [9] Kamaruddin K, Hassan S, Ashaary Ahmad AFI, Lajis MA, and Rahim EA. Study on tool wear and wear mechanisms of end milling nickel-based alloy. *J Tribol*, 21:82–92, 2019.
- [10] Ucun I, Aslantas K, and Bedir F. An experimental investigation of the effect of coating material on tool wear in micro milling of inconel 718 super alloy. *Wear*, 300(1-2):8–19, 2013.
- [11] Pleta A, Ulutan D, and Mears L. Investigation of trochoidal milling in nickel-based superalloy Inconel 738 and comparison with end milling. In *International Manufacturing Science and Engineering Conference*, volume 45813, page V002T02A058. American Society of Mechanical Engineers, 2014.
- [12] Altin A, Nalbant M, and Taskesen A. The effects of cutting speed on tool wear and tool life when machining Inconel 718 with ceramic tools. *Materials & design*, 28(9):2518–2522, 2007.
- [13] Niaki FA, Ulutan D, and Mears L. Stochastic tool wear assessment in milling difficult to machine alloys. *International Journal of Mechatronics* and Manufacturing Systems, 8(3-4):134–159, 2015.

- [14] Attanasio A, Faini F, and Outeiro JC. FEM simulation of tool wear in drilling. *Procedia Cirp*, 58:440–444, 2017.
- [15] Fan YH, Wang T, Hao ZP, Lan H, and Cui RR. Research on tool wear based on multi-scale simulation in high speed cutting Inconel718. Archives of Civil and Mechanical Engineering, 18(3):928–940, 2018.
- [16] Bergmann JA, Potthoff N, Rickhoff T, and Wiederkehr P. Modeling of cutting forces in trochoidal milling with respect to wear-dependent topographic changes. *Production Engineering*, pages 1–9, 2021.
- [17] Grimm T, Potthoff N, Kharat N, Mears L, and Wiederkehr P. Development of a contrived tool wear method in machining. In *Proceedings of ASME International Mechanical Engineering Conference and Exposition*, 2021 (in press).
- [18] Bleicher F, Ramsauer CM, Oswald R, Leder N, and Schoerghofer P. Method for determining edge chipping in milling based on tool holder vibration measurements. CIRP Annals, 69(1):101–104, 2020.
- [19] Potthoff N and Wiederkehr P. Fundamental investigations on wear evolution of machining Inconel 718. Procedia CIRP, 99C:171–176, 2021.
- [20] Ducobu F, , Rivière-Lorphèvre E, and Filippi E. Application of the coupled eulerian-lagrangian (cel) method to the modeling of orthogonal cutting. *European Journal of Mechanics-A/Solids*, 59:58–66, 2016.
- [21] Ducobu F, Arrazola PJ, Rivière-Lorphèvre E, de Zarate GO, Madariaga A, and Filippi E. The cel method as an alternative to the current modelling approaches for ti6al4v orthogonal cutting simulation. *Procedia Cirp*, 58:245– 250, 2017.
- [22] Melkote SN, Grzesik W, Outeiro J, Rech J, Schulze V, Attia H, Arrazola PJ, M'Saoubi R, and Saldana C. Advances in material and friction data for modelling of metal machining. *Cirp Annals*, 66(2):731–754, 2017.
- [23] Klocke F, Döbbeler B, Peng B, and Schneider SAM. Tool-based inverse determination of material model of direct aged alloy 718 for fem cutting simulation. *Procedia CIRP*, 77:54–57, 2018.